RSC Advances

PAPER

View Article Online
View Journal | View Issue

Cite this: *RSC Adv.*, 2023, **13**, 23538

Design, synthesis and antiproliferative screening of newly synthesized acrylate derivatives as potential anticancer agents†

Dalal Sulaiman Alshaya,[a] Rana M. O. Tawakul,[b] Islam Zaki, *[c] Ali H. Abu Almaaty,[b] Eman Fayad[d] and Yasmin M. Abd El-Aziz[b]

Received 8th June 2023
Accepted 19th July 2023

DOI: 10.1039/d3ra03849a

rsc.li/rsc-advances

A new series of acrylic acid and acrylate ester derivatives as modified analogs of tubulin polymerization inhibitors were designed and synthesized. The antiproliferative activity of the constructed molecules was investigated against MCF-7 breast carcinoma cells using CA-4 as positive molecule. Methyl acrylate ester **6e** emerged as the most potent cytotoxic agent against MCF-7 cells, with an IC_{50} value of 2.57 ± 0.16 μM. Also, methyl acrylate ester molecule **6e** showed good β-tubulin polymerization inhibition activity. Cellular cycle analysis showed that compound **6e** can arrest MCF-7 cells at the G2/M phase. In addition, this compound produced a significant increase in apoptotic power as compared to control untreated MCF-7 cells. Furthermore, the effect of acrylate ester **6e** on the gene expression levels of p53, Bax and Bcl-2 was investigated. This molecule increased the expression levels of both p53 and Bax, and decreased the gene expression level of Bcl-2 as compared to control untreated MCF-7 carcinoma cells.

1. Introduction

The importance of microtubule polymerization in cancer control has been emphasized.[1,2] Microtubule formation, comprising α/β tubulin heterodimers, has a crucial role in cellular processes such as maintaining cellular shape and cellular division of eukaryotic cells and is therefore regarded as an outstanding molecular target for chemotherapy.[3–5] Tubulin polymerization is required for microtubule formation.[6] Tubulin assembly inhibitors interfere with the tubulin-microtubule polymerization–depolymerization process and are becoming an attractive strategy for the development of highly efficient anticancer drugs.[7–9] Several natural products, such as colchicine, paclitaxel, and the vinca alkaloids, inhibit tubulin polymerization by binding to tubulin at their respective binding sites.[10,11] In the case of tubulin polymerization inhibition at the colchicine binding site, combretastatin A-4 (CA-4) is a *cis*-stilbenoid molecule that elicited remarkable β-tubulin polymerization suppression activity acting at the colchicine site.[12–14] CA-4 is the lead antimitotic molecule within the combretastatin family which exerts outstanding antitumor activity on various cancer cells due to β-tubulin polymerization suppression activity and anti-vascular effect.[15,16] This is in addition to its potency against multidrug resistant cancer cell line.[17] A property that makes analogs of CA-4 attractive for further development of more appropriate anticancer molecules which could be utilized in clinical use to overcome the drawbacks of conventional anticancer regimens, especially development of drug resistance.[18–20]

Acrylate moiety is a common structural scaffold in the structure of numerous natural and synthetic small compounds displaying versatile biological interests.[21,22] It has been reported to exhibit diverse biomedical activities, including anticancer activity.[23] Their development has introduced new molecules acting as anticancer agents through different mechanisms such as β-tubulin inhibition and protein kinase inhibition.[24,25] These findings suggested that acrylate pharmacophore is a promising molecular scaffold for further modification to develop more effective anticancer drug candidates.[26]

The two most frequently utilized methods in medicinal chemistry in the design of novel molecules are bioisosterism and molecular hybridization.[27] The isosteric modification method is an efficient and often used technique that many drug candidates employ to enhance their pharmacodynamic behavior.[28] It was of interest to further exploit the lead antimitotic agent, CA-4, with the possibility of producing effective drugs active against breast carcinoma cells.[29] Encouraged by the above findings, we desired to design and synthesize a new series of acrylic acids and acrylate esters-containing scaffolds in the hope of getting more potent congeners (Fig. 1). The synthesized

[a]*Department of Biology, College of Science, Princess Nourah bint Abdulrahman University, P.O. Box 84428, Riyadh 11671, Saudi Arabia*
[b]*Zoology Department, Faculty of Science, Port Said University, Port Said 42526, Egypt*
[c]*Pharmaceutical Organic Chemistry Department, Faculty of Pharmacy, Port Said University, Port Said 42526, Egypt. E-mail: Eslam.Zaki@pharm.psu.edu.eg*
[d]*Department of Biotechnology, Faculty of Sciences, Taif University, P.O. Box 11099, Taif 21944, Saudi Arabia*

† Electronic supplementary information (ESI) available. See DOI: https://doi.org/10.1039/d3ra03849a

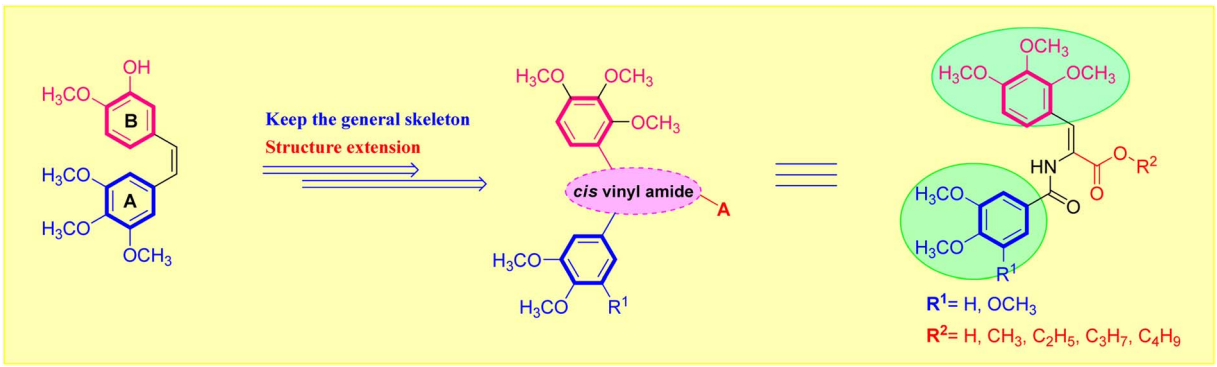

Fig. 1 Designed strategy of the target acrylate derivatives **5a,b** and **6a–i**. A = carboxylic acid or ester group.

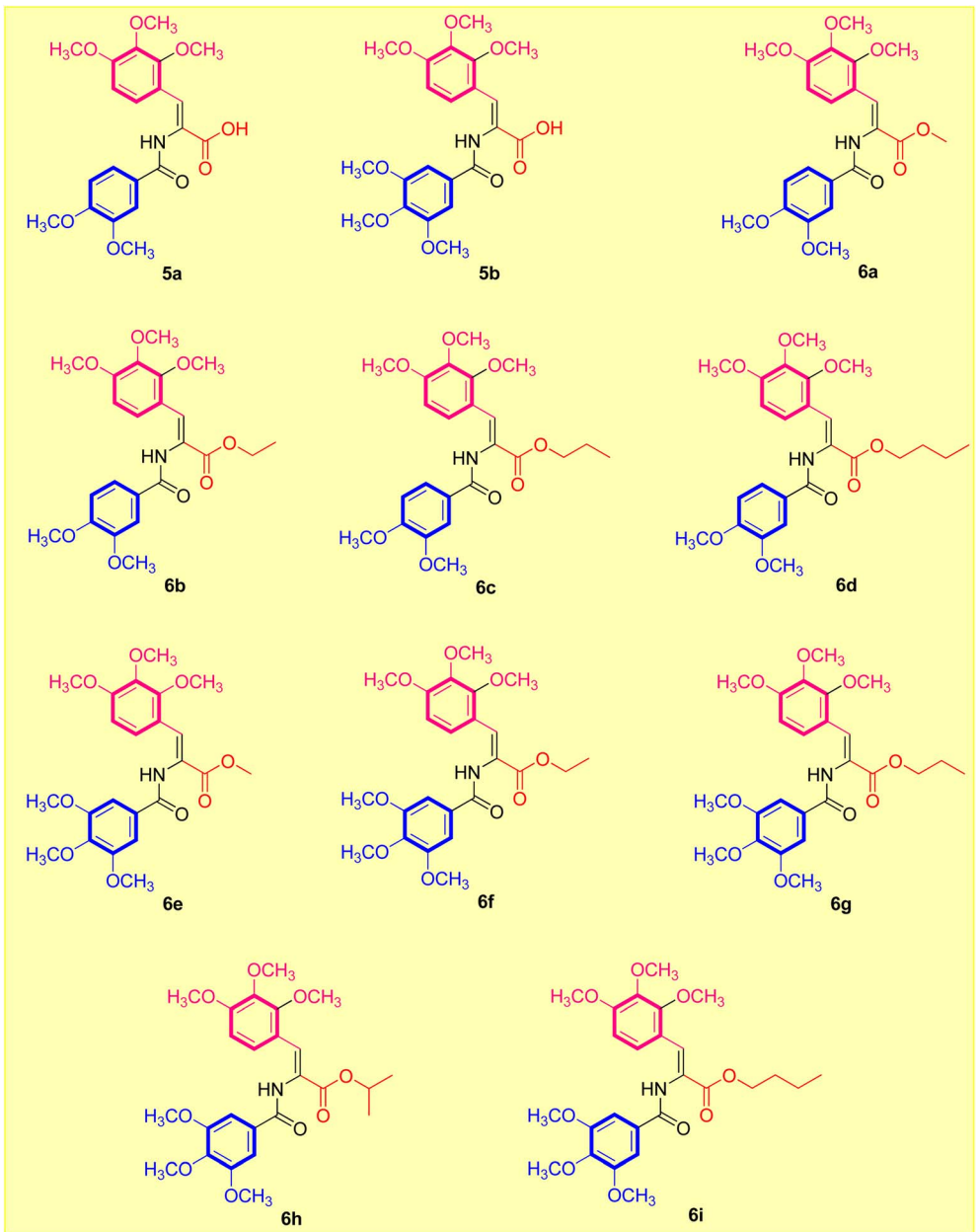

Fig. 2 Designed acrylate compounds (**5a,b** and **6a–i**) in the current study.

molecules were evaluated *in vitro* against MCF-7 breast cancer cells to assess their cytotoxic and β-tubulin polymerization inhibition activities (Fig. 2).

2. Results and discussion

2.1. Chemistry

The targeted novel derivatives **5a,b** and **6a–i** were synthesized as depicted in Scheme 1. To prepare the key intermediates **4a,b**, the Knoevenagel reaction was utilized. 2,3,4-Trimethoxybenzaldehyde was condensed with Respective hippuric acid **3a,b** by refluxing in a solution of sodium acetate and acetic anhydride to give the desired (*Z*)-2-aryl-4-(2,3,4-trimethoxybenzylidene)oxazol-5(4*H*)-ones **4a,b.**

Consequently, treatment of compound **4a,b** with aqueous K_2CO_3 for 3–4 h followed by neutralization in acidic solution afforded the corresponding carboxylic acid derivative **5a,b**. The ^{1}H-NMR spectrum of acrylic acid compound **5b** showed two

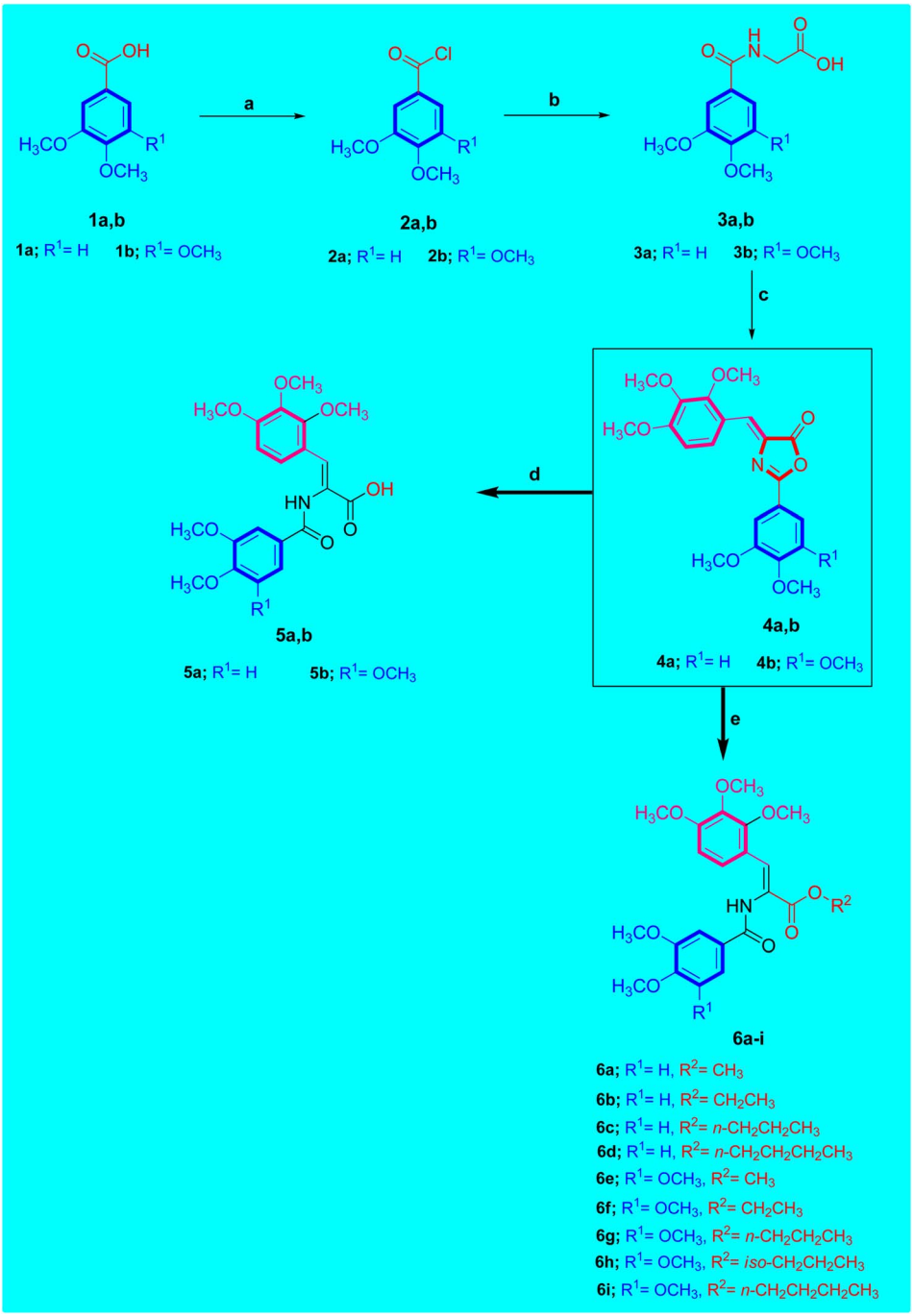

Scheme 1 Synthetic approach of acrylate compounds **5a,b** and **6a–i**. Reagents: (a) $SOCl_2$, CH_2Cl_2, reflux 2 h; (b) glycine, Et_3N, CH_3CN/H_2O, stirring, r.t.; (c) 2,3,4-*tri*-OCH_3-C_6H_2CHO, NaOAc, Ac_2O, 80 °C 2 h; (d) KOH, H_2O, reflux 3–4 h; (e) respective aliphatic alcohol, Et_3N, reflux 2–3 h.

singlet signals at δ 12.65 and 9.75 ppm corresponding to OH proton of carboxylic acid moiety and NH proton of amide function, respectively. The aromatic protons of the 2,3,4-trimethoxybenzylidene ring of compound **5b** resonated as two doublet signals at δ 7.44 and 6.85 ppm integrating for one proton for each signal, respectively. In addition, the aromatic protons of 3,4,5-trimethoxyphenyl ring of compound **5b** resonated as singlet signal at δ 7.32 ppm integrating for two protons. The olefinic proton resonated as singlet peak at δ 7.57 ppm integrating for one proton. Furthermore, ^{13}C-NMR spectrum of acrylic acid compound **5b** showed five peaks at δ 61.92, 60.90, 60.57, 56.52 and 56.42 ppm corresponding to six methoxy groups of 2,3,4-trimethoxybenzylidene in addition to 3,4,5-trimethoxyphenyl moieties and two peaks at δ 162.66 and 163.77 ppm related to two carbonyl groups (C=O) of carboxylic acid and amide moieties, respectively.

Treating compound **4a,b** with respective alcohol; namely methyl alcohol, ethyl alcohol, propyl alcohol, iso-propyl alcohol or *n*-butyl alcohol in the presence of triethyl amine (Et_3N) yielded the desired ester derivative **6a–i**. Concerning ester derivatives **6a–i**, single peak corresponding to amide (NH) group was found in the ^{1}H-NMR spectrum between δ 9.91 and 9.79 ppm. For example, consider compound **6g** which was designated as (*Z*)-propyl 2-(3,4,5-trimethoxybenzamido)-3-(2,3,4-trimethoxyphenyl) acrylate $C_{25}H_{33}NO_9$ showed the presence of two singlet peaks at 9.88 and 7.53 ppm corresponding to amidic NH and olefinic protons, respectively. In this respect, the ^{1}H-NMR spectrum of compound **6g** revealed three sets of protons resonated as triplet at δ 4.11, sextet at δ 1.65 and as triplet at δ 0.91 ppm integrating for 2H, 2H, and 3H, respectively which was attributed to propyl function ($OCH_2CH_2CH_3$). ^{13}C-NMR spectrum of compound **6g** confirmed the carbon skeleton due to the presence of three signals at δ 66.64, 22.08 and 10.75 ppm corresponding to propyl group ($OCH_2CH_2CH_3$), in addition to five peaks at δ 61.94, 60.94, 60.56, 56.52 and 56.44 ppm corresponding to six methoxy (OCH_3) functions. Furthermore, ^{13}C-NMR spectrum of compound **6g** revealed the presence of two singlet peaks at δ 165.91 and 165.58 ppm due to carbonyl groups (C=O) of ester and amide moieties respectively.

2.2. Biology

2.2.1. Cytotoxic activity against MCF-7 breast cancer cell line. Cytotoxic activity of the synthesized acrylate derivatives **5a–6i** was evaluated against the MCF-7 breast carcinoma cell line using the MTT colorimetric assay. CA-4 was included as a positive control. The results were summarized as IC_{50} values in Table 1. From the presented results, it was found that the tested acrylate derivatives **5a–6i** showed considerable cytotoxic activity against MCF-7 cells with IC_{50} values 2.57–42.08 μM. Compounds **5b** (IC_{50} = 5.12 μM), **6a** (IC_{50} = 6.74 μM), **6e** (IC_{50} = 2.57 μM), **6f** (IC_{50} = 3.26 μM) and **6h** (IC_{50} = 7.08 μM) were the most active molecules against MCF-7 cells. From the obtained results, compound **6e** (IC_{50} = 2.57 μM) emerged as the most active member of the synthesized acrylate derivatives. In the acrylic acid analogs **5a,b**, compound **5b** (IC_{50} = 5.12 μM) bearing 3,4,5-trimethoxyphenyl and 2,3,4-trimethoxybenzylidene moieties displayed better cytotoxic activity than compound **5a** (IC_{50} = 9.31 μM) bearing 3,4-dimethoxyphenyl and 2,3,4-trimethoxybenzylidene groups. Regarding the acrylate ester derivatives **6a–i**, it can be observed that the methyl acrylate ester compound **6e** (IC_{50} = 2.57 μM) exerted good cytotoxic activity and was the most active compound compared with its methyl acrylate ester congeners **6a** (IC_{50} = 6.74 μM) or other alkyl substituted derivatives.

Table 1 *In vitro* cytotoxic activity of the synthesized acrylic acids **5a,b** and acrylate esters **6a–i** against MCF-7 breast carcinoma cell line[a]

Comp. no.	IC_{50} value (μM)	
	MCF-7	MCF-10A
5a	9.31 ± 0.35	NT
5b	5.12 ± 0.32	NT
6a	6.74 ± 0.78	NT
6b	17.08 ± 0.49	NT
6c	20.26 ± 0.44	NT
6d	42.08 ± 0.96	NT
6e	2.57 ± 0.16	19.06 ± 0.31
6f	3.26 ± 0.21	NT
6g	11.34 ± 0.75	NT
6h	7.08 ± 0.29	NT
6i	33.02 ± 1.03	NT
CA-4	1.25 ± 0.08	13.18 ± 0.19

[a] NT; not tested.

2.2.2. Tubulin assay. The disruption of the cellular microtubule structure and, more importantly, microtubule function that result from inhibiting β-tubulin polymerization leads to the triggering of cellular apoptosis.[30,31] Inhibition of tubulin polymerization has been identified as a possible therapeutic target for the creation of new cancer therapies.[32] The most potent cytotoxic acrylate ester molecule **6e** was assessed for its β-

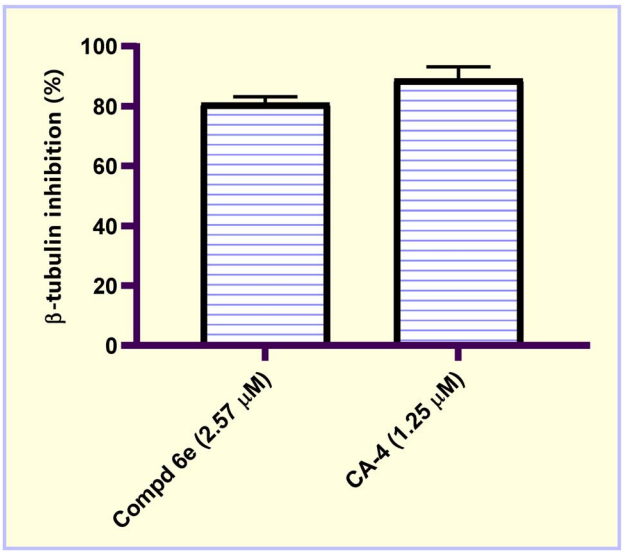

Fig. 3 Graphical representation of β-tubulin inhibition (%) in MCF-7 breast carcinoma cells after treatment with methyl acrylate ester **6e** and CA-4 at the IC_{50} concentration (μM).

tubulin polymerization inhibition activity using CA-4 as a reference compound. This compound was tested at a concentration equal to its IC_{50} dose value (IC_{50} = 2.57 μM) for 48 h utilizing MCF-7 breast carcinoma cells. The results were presented as percent inhibition values, as shown in Fig. 3. The results showed that, as compared to untreated control cells, the tested acrylate ester compound **6e** produced a 5.73-fold decrease in the level of β-tubulin polymerization. In addition, compared to CA-4 (89.17% polymerization inhibition), acrylate ester molecule **6e** showed good β-tubulin polymerization inhibition activity with β-tubulin inhibition percentage of 81.16%. These results showed that the molecular target of acrylate ester molecule **6e** may be tubulin.

2.2.3. Cell cycle analysis. Tubulin polymerization inhibitors have demonstrated effectiveness in disrupting cellular cycle stages, resulting in cellular cycle arrest and cell death.[33] To demonstrate the checkpoint at which the synthesized acrylate compounds block cellular growth, a cell cycle assay was carried out for the most active ester candidate, **6e**. This compound was tested at a concentration equal to its IC_{50} dose value (IC_{50} = 2.57 μM) for 48 h utilizing MCF-7 breast carcinoma cells. It can be shown that methyl acrylate compound **6e** revealed a significant decrease in the cellular population in the G1 and S phases from 54.92 and 26.88%, respectively (in control untreated cells) to 47.98 and 22.06%, respectively (in treated cells). On the other hand, the cell population increased in the G2/M phase from 8.20% (in control untreated cells) to 29.96% (in the treated cells) (Fig. 4). These findings indicated that methyl acrylate compound **6e** arrested the MCF-7 breast carcinoma cells at the G2/M phase checkpoint.

2.2.4. Apoptosis analysis. Apoptosis is vital for maintaining proper tissue homeostasis within mature organisms.[34] Apoptosis inhibition can contribute to the onset and spread of cancer, so apoptosis activation in cancer cells may have positive benefits in cancer chemotherapy.[35] Fluorochrome Annexin-V/propidium iodide (PI) staining (Annexin-V/FITC) was performed to assess the apoptotic activity of the most active

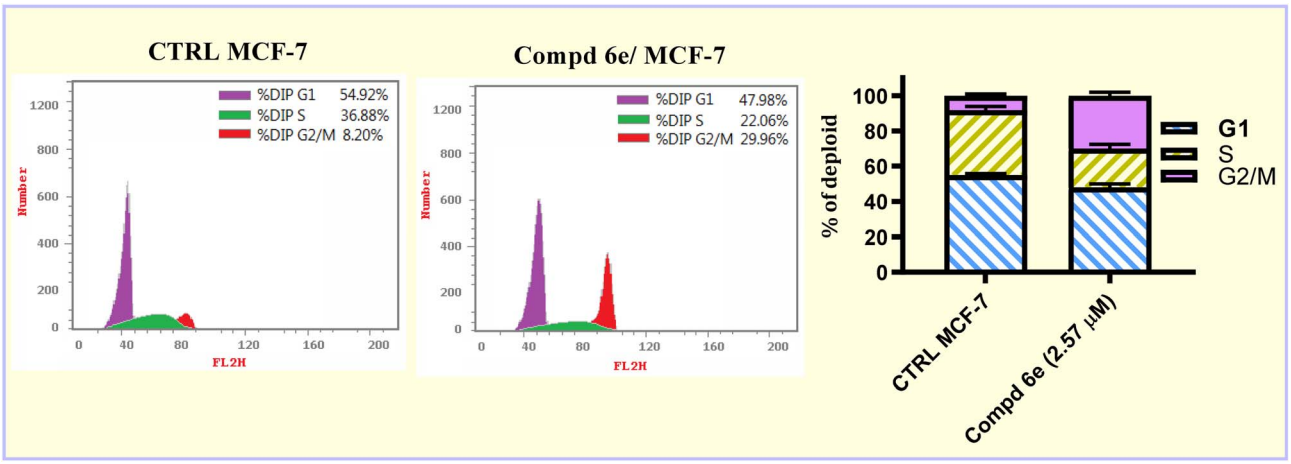

Fig. 4 Flow cytometric cell cycle analysis of MCF-7 breast carcinoma cells before and after 48 h treatment with 2.57 μM of methyl acrylate ester **6e**.

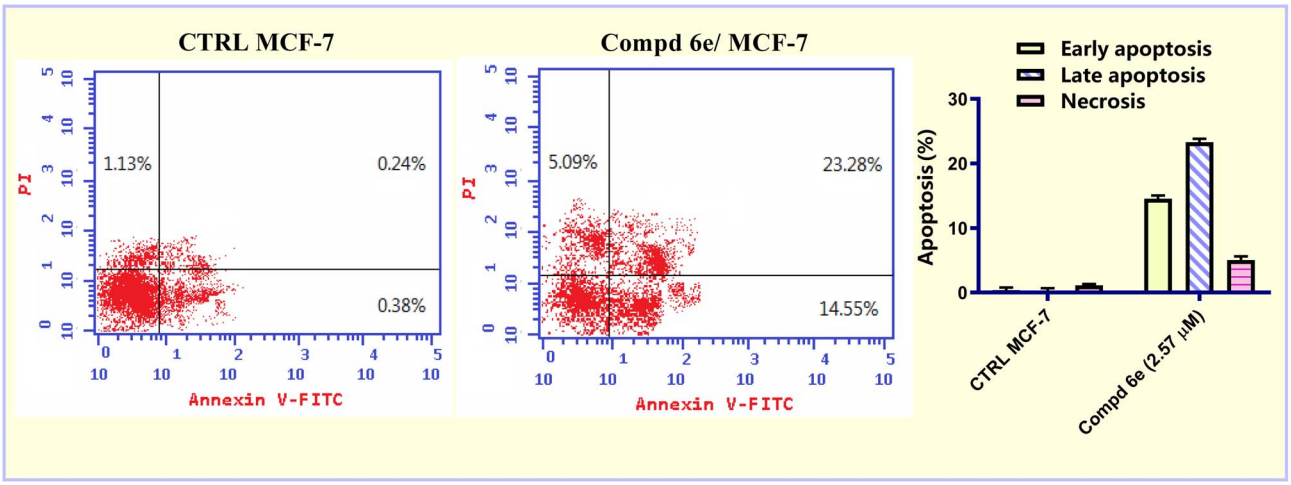

Fig. 5 The impact of methyl acrylate ester **6e** on the percentage of Annexin V-FITC positive staining in breast carcinoma MCF-7 cells before and after 48 h treatment with 2.57 μM.

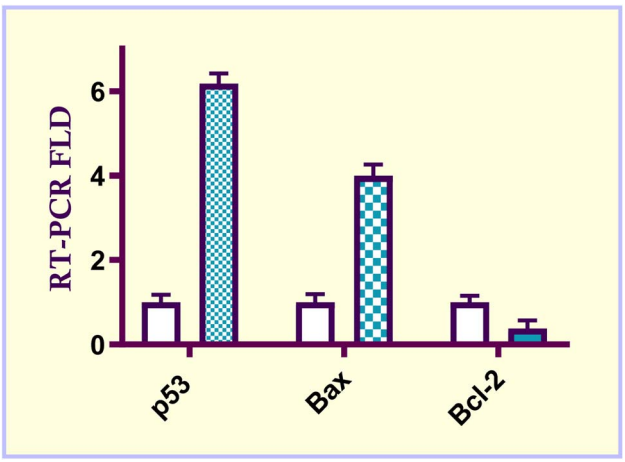

Fig. 6 Effect of methyl acrylate ester **6e** (IC_{50} = 2.57 μM) on the gene expression of apoptosis-associated markers before and after a 48 h treatment in MCF-7 breast carcinoma cells.

acrylate ester derivative **6e**, utilizing MCF-7 breast carcinoma cells at a concentration of 2.57 μM for 48 h. The results in Fig. 5 demonstrated that, methyl acrylate ester **6e** showed a significant increase in apoptotic activity. For the early stage, the apoptotic cells increased from 0.38% (in the control untreated cells) to 14.55% (in the treated cells). Regarding the late stage, the apoptotic cells increased from 0.24% (in the control untreated cells) to 23.28% (in the treated cells). These results revealed that acrylate ester **6e** produced a 49.27-fold increase in the apoptotic cells compared to the control untreated MCF-7 breast carcinoma cells.

2.2.5. *In vitro* gene expression measurement for p53, Bax and Bcl-2. p53, Bax and Bcl-2 play a key role in controlling intrinsic mitochondrial cellular death.[36] Molecular control of the apoptotic process may ultimately lead to the development of more potent therapies for cancer.[37] During the apoptotic process, these mediators have opposing effects. p53 and Bax have proapoptotic impacts, while Bcl-2 has anti-apoptotic effects. At a dose value of 2.57 μM, the most active ester derivative **6e** was tested for its intrinsic apoptosis in MCF-7 breast carcinoma cells. This assay utilized the quantitative real time reverse transcriptase PCR (qRT-PCR) assay. The data indicated that methyl acrylate ester derivatives **6e** upregulate p53 level by 6.18-fold higher than untreated control cells. Similarly, acrylate ester compound **6e** increased Bax level by 3.99-fold relative to untreated control cells. On the other hand, compound **6e** decreased the level of anti-apoptotic gene Bcl-2 level by 0.38-fold less than untreated cells. Subsequently, compound **6e** increased the ratio of Bax/Bcl-2 by 10.5-fold as compared to untreated cells. These findings demonstrated that the methyl acrylate ester derivative **6e** has a strong apoptotic impact on the intrinsic mitochondrial apoptotic pathway (Fig. 6).

3. Conclusions

In the current study, a new series of acrylic acid and acrylate ester derivatives structurally related to CA-4 were designed and synthesized. The chemical structures of the constructed acrylate derivatives were substantiated on the basis of ^{1}H-NMR, ^{13}C-NMR spectroscopic studies and elemental analyses. The results revealed that methyl acrylate compound **6e** (IC_{50} = 2.57 ± 0.16 μM) was the most potent against the MCF-7 breast carcinoma cell line. Methyl acrylate molecule **6e** showed good β-tubulin polymerization inhibition activity (81.16% polymerization inhibition) relative to CA-4 as a positive control (82.82% polymerization inhibition). Compound **6e** exerted an increase in the percentage of MCF-7 cells at the G2/M phase from 8.20% to 29.96% compared to the untreated control. In addition, methyl acrylate molecule **6e** elicited a significant increase in the apoptotic power of MCF-7 cells. In the early stage from 0.38% to 14.55% and in the late stage from 0.24% to 23.28% compared to the untreated control. Moreover, compound **6e** boosted the gene expression levels of both p53, Bax by 6.18- and 3.99-fold, respectively, relative to the untreated control. On the other hand, it caused a significant reduction in the Bcl-2 gene expression level by 0.38-fold relative to untreated MCF-7 breast carcinoma cells.

4. Experimental

4.1. Synthesis

4.1.1. General method of synthesis of (*Z*)-2-aryl-3-(2,3,4-trimethoxyphenyl)acrylic acids (5a,b). Respective oxazolone derivatives **4a,b** (0.0015 mol) was heated with KOH in distilled water (30 mL) for 3–4 h, till formation of the corresponding potassium salt. The reaction was filtered while hot and the filtrate thus obtained was neutralized with HCl (2 N). The obtained precipitate was filtered, dried and crystallized from aqueous ethanol (70%) to afford acrylic acid **5a,b**.

*4.1.1.1 (Z)-2-(3,4-Dimethoxybenzamido)-3-(2,3,4-trimethoxyphenyl)acrylic acid (**5a**).* White powder (0.30 g, 48%), mp 201–203 °C. ^{1}H-NMR (400 MHz, DMSO-d_6, δ ppm): 12.60 (s, 1H, OH), 9.65 (s, 1H, NH), 7.65–7.59 (m, 1H, arom. CH), 7.55 (s, 2H, arom. CH and olefinic CH), 7.44 (d, J = 8.9 Hz, 1H, arom. CH), 7.07 (d, J = 8.5 Hz, 1H, arom. CH), 6.83 (d, J = 9.0 Hz, 1H, arom. CH), 3.85 (s, 3H, OCH_3), 3.84 (s, 3H, OCH_3), 3.82 (s, 3H, OCH_3), 3.79 (s, 3H, OCH_3), 3.76 (s, 3H, OCH_3). ^{13}C-NMR (100 MHz, DMSO-d_6, δ ppm): 167.07, 165.80, 154.93, 152.79, 152.15, 148.77, 142.00, 127.26, 126.82, 126.29, 124.44, 121.55, 120.64, 111.43, 111.42, 108.57, 61.92, 60.91, 56.40, 56.14, 56.04. Anal. calcd for $C_{21}H_{23}NO_8$ (417.41): C, 60.43; H, 5.55; N, 3.36. Found: C, 60.32; H, 5.42; N, 3.44.

*4.1.1.2 (Z)-2-(3,4,5-Trimethoxybenzamido)-3-(2,3,4-trimethoxyphenyl)acrylic acid (**5b**).* White powder (0.29 g, 43%), mp 217–219 °C. ^{1}H-NMR (400 MHz, DMSO-d_6, δ ppm): 12.65 (s, 1H, OH), 9.75 (s, 1H, NH), 7.57 (s, 1H, olefinic CH), 7.44 (d, J = 8.9 Hz, 1H, arom. CH), 7.32 (s, 2H, arom. CH), 6.85 (d, J = 9.0 Hz, 1H, arom. CH), 3.86 (s, 3H, OCH_3), 3.85 (s, 6H, $2OCH_3$), 3.79 (s, 3H, OCH_3), 3.76 (s, 3H, OCH_3), 3.73 (s, 3H, OCH_3). ^{13}C-NMR (100 MHz, DMSO-d_6, δ ppm): 166.95, 165.64, 155.00, 153.12, 152.81, 142.01, 140.86, 129.10, 127.36, 126.60, 124.45, 120.53, 108.63, 105.73, 61.92, 60.90, 60.57, 56.52, 56.42. Anal. calcd for $C_{22}H_{25}NO_9$ (447.44): C, 59.06; H, 5.63; N, 3.13. Found: C, 58.85; H, 5.87; N, 3.19.

4.1.2. General method of synthesis of (*Z*)-2-aryl-3-(2,3,4-trimethoxyphenyl)acrylate esters (6a–i). A mixture of respective oxazolone derivatives **4a,b** (0.0015 mol) and 25 mL of suitable aliphatic alcohol; namely methyl alcohol, ethyl alcohol, *n*-propyl alcohol, isopropyl alcohol and *n*-butyl alcohol contain triethyl amine (10 drops) was refluxed for 2–3 h. After reaction accomplishment, the reaction mixture was cooled and poured on crushed ice. The formed precipitate was filtered, dried and crystallized from ethanol (70%) to afford acrylate ester compounds **6a–i**.

*4.1.2.1 (Z)-Methyl 2-(3,4-dimethoxybenzamido)-3-(2,3,4-trimethoxyphenyl)acrylate (**6a**).* White powder (0.45 g, 69%), mp 177–179 °C. ^{1}H-NMR (400 MHz, DMSO-d_6, δ ppm): 9.81 (s, 1H, NH), 7.63 (d, J = 8.4 Hz, 1H, arom. CH), 7.55 (s, 1H, olefinic CH), 7.51 (s, 1H, arom. CH), 7.44 (d, J = 8.9 Hz, 1H, arom. CH), 7.08 (d, J = 8.4 Hz, 1H, arom. CH), 6.85 (d, J = 9.0 Hz, 1H), 3.86 (s, 3H, OCH_3), 3.84 (s, 3H, OCH_3), 3.83 (s, 3H, OCH_3), 3.80 (s, 3H, OCH_3), 3.76 (s, 3H, OCH_3), 3.73 (s, 3H, OCH_3). ^{13}C-NMR (100 MHz, DMSO-d_6, δ ppm): 166.22, 165.91, 155.15, 152.88, 152.29, 148.83, 142.02, 127.37, 126.06, 125.95, 124.53, 121.61, 120.31, 111.48, 111.41, 108.62, 61.96, 60.91, 56.44, 56.16, 56.05, 52.65. Anal. calcd for $C_{22}H_{25}NO_8$ (431.44): C, 61.25; H, 5.84; N, 3.25. Found: C, 61.33; H, 6.04; N, 3.13.

*4.1.2.2 (Z)-Ethyl 2-(3,4-dimethoxybenzamido)-3-(2,3,4-trimethoxyphenyl)acrylate (**6b**).* White powder (0.41 g, 61%), mp 154–156 °C. ^{1}H-NMR (400 MHz, DMSO-d_6, δ ppm): 9.78 (s, 1H, NH), 7.68–7.60 (m, 1H, arom. CH), 7.55 (s, 1H, olefinic CH), 7.50 (s, 1H, arom. CH), 7.45 (d, J = 8.5 Hz, 1H, arom. CH), 7.08 (d, J = 7.7 Hz, 1H, arom. CH), 6.85 (d, J = 8.4 Hz, 1H, arom. CH), 4.19 (q, J = 1.6 Hz, 2H, OCH_2CH_3), 3.86 (s, 3H, OCH_3), 3.84 (s, 3H, OCH_3), 3.83 (s, 3H, OCH_3), 3.80 (s, 3H, OCH_3), 3.76 (s, 3H, OCH_3), 1.23 (t, J = 1.3 Hz, 3H, OCH_2CH_3). ^{13}C-NMR (100 MHz, DMSO-d_6, δ ppm): 165.95, 165.66, 155.08, 152.86, 152.25, 148.82, 142.02, 127.06, 126.38, 126.09, 124.53, 121.57, 120.39, 111.48, 111.39, 108.60, 61.95 (OCH_2CH_3), 61.19, 60.91, 56.42, 56.15, 56.05, 14.62 (OCH_2CH_3). Anal. calcd for $C_{23}H_{27}NO_8$ (445.46): C, 62.01; H, 6.11; N, 3.14. Found: C, 61.88; H, 6.16; N, 3.02.

*4.1.2.3 (Z)-Propyl 2-(3,4-dimethoxybenzamido)-3-(2,3,4-trimethoxyphenyl)acrylate (**6c**).* White powder (0.44 g, 64%), mp 119–121 °C. ^{1}H-NMR (400 MHz, DMSO-d_6, δ ppm): 9.79 (s, 1H, NH), 7.62 (d, J = 7.0 Hz, 1H, arom. CH), 7.54 (s, 1H, olefinic CH), 7.51 (s, 1H, arom. CH), 7.46 (d, J = 8.9 Hz, 1H, arom. CH), 7.08 (d, J = 8.5 Hz, 1H, arom. CH), 6.85 (d, J = 9.0 Hz, 1H, arom. CH), 4.10 (t, J = 6.4 Hz, 2H, $OCH_2CH_2CH_3$), 3.85 (s, 3H, OCH_3), 3.84 (s, 3H, OCH_3), 3.82 (s, 3H, OCH_3), 3.80 (s, 3H, OCH_3), 3.76 (s, 3H, OCH_3), 1.62 (h, J = 7.0 Hz, 2H, $OCH_2CH_2CH_3$), 0.90 (t, J = 7.4 Hz, 3H, $OCH_2CH_2CH_3$). ^{13}C-NMR (100 MHz, DMSO-d_6, δ ppm): 166.03, 165.73, 155.10, 152.87, 152.23, 148.80, 142.04, 127.09, 126.37, 126.12, 124.55, 121.56, 120.38, 111.48, 111.38, 108.64, 66.59 ($OCH_2CH_2CH_3$), 61.94, 60.92, 56.43, 56.15, 56.05, 22.08 ($OCH_2CH_2CH_3$), 10.76 ($OCH_2CH_2CH_3$). Anal. calcd for $C_{24}H_{29}NO_8$ (459.49): C, 62.73; H, 6.36; N, 3.05. Found: C, 62.86; H, 6.29; N, 2.93.

*4.1.2.4 (Z)-Butyl 2-(3,4-dimethoxybenzamido)-3-(2,3,4-trimethoxyphenyl)acrylate (**6d**).* White powder (0.37 g, 52%), mp 132–134 °C. ^{1}H-NMR (400 MHz, DMSO-d_6, δ ppm): 9.81 (s, 1H, NH), 7.66–7.60 (m, 1H, arom. CH), 7.57–7.53 (m, 1H, arom. CH), 7.51 (s, 1H, olefinic CH), 7.44 (d, J = 9.0 Hz, 1H, arom. CH), 7.08 (d, J = 8.5 Hz, 1H, arom. CH), 6.85 (d, J = 9.0 Hz, 1H, arom. CH), 4.31–3.91 (m, 2H, $OCH_2CH_2CH_2CH_3$), 3.86 (s, 3H, OCH_3), 3.84 (s, 3H, OCH_3), 3.83 (s, 3H, OCH_3), 3.80 (s, 3H, OCH_3), 3.76 (s, 3H, OCH_3), 3.73 (s, 2H, $OCH_2CH_2CH_2CH_3$), 1.62 (q, J = 6.9 Hz, 2H, $OCH_2CH_2CH_2CH_3$), 0.90 (t, J = 7.4 Hz, 3H, $OCH_2CH_2CH_2CH_3$). ^{13}C-NMR (100 MHz, DMSO-d_6, δ ppm): 166.22, 165.91, 155.15, 152.88, 152.29, 148.83, 142.02, 127.36, 126.06, 125.96, 124.53, 121.61, 120.31, 111.48, 111.41, 108.62, 66.59 ($OCH_2CH_2CH_2CH_3$), 61.96, 60.91, 56.44, 56.16, 56.05, 52.65 ($OCH_2CH_2CH_2CH_3$), 22.09 ($OCH_2CH_2CH_2CH_3$), 10.76 ($OCH_2CH_2CH_2CH_3$). Anal. calcd for $C_{25}H_{31}NO_8$ (473.52): C, 63.41; H, 6.60; N, 2.96. Found: C, 63.26; H, 6.68; N, 3.08.

*4.1.2.5 (Z)-Methyl 2-(3,4,5-trimethoxybenzamido)-3-(2,3,4-trimethoxyphenyl)acrylate (**6e**).* White powder (0.50 g, 72%), mp 133–135 °C. ^{1}H-NMR (400 MHz, DMSO-d_6, δ ppm): 9.91 (s, 1H, NH), 7.53 (s, 1H, olefinic CH), 7.44 (d, J = 8.9 Hz, 1H, arom. CH), 7.33 (s, 2H, arom. CH), 6.87 (d, J = 9.0 Hz, 1H, arom. CH), 3.86 (s, 3H, OCH_3), 3.85 (s, 6H, $2OCH_3$), 3.80 (s, 3H, OCH_3), 3.76 (s, 3H, OCH_3), 3.74 (s, 6H, $2OCH_3$). ^{13}C-NMR (100 MHz, DMSO-d_6, δ ppm): 166.10, 165.76, 155.23, 153.17, 152.91, 142.02, 140.99, 128.75, 127.48, 125.82, 124.55, 120.18, 108.68, 105.77, 61.97, 60.91, 60.57, 56.53, 56.45, 52.70. Anal. calcd for $C_{23}H_{27}NO_9$ (461.46): C, 59.86; H, 5.90; N, 3.04. Found: C, 59.98; H, 5.81; N, 2.93.

*4.1.2.6 (Z)-Ethyl 2-(3,4,5-trimethoxybenzamido)-3-(2,3,4-trimethoxyphenyl)acrylate (**6f**).* White powder (0.51 g, 71%), mp 127–129 °C. ^{1}H-NMR (400 MHz, DMSO-d_6, δ ppm): 9.87 (s, 1H, NH), 7.50 (s, 1H, olefinic CH), 7.44 (d, J = 8.9 Hz, 1H, arom. CH), 7.31 (s, 2H, arom. CH), 6.86 (d, J = 9.0 Hz, 1H, arom. CH), 4.19 (q, J = 7.1 Hz, 2H, OCH_2CH_3), 3.85 (s, 3H, OCH_3), 3.84 (s, 6H, $2OCH_3$), 3.79 (s, 3H, OCH_3), 3.75 (s, 3H, OCH_3), 3.73 (s, 3H, OCH_3), 1.23 (t, J = 7.1 Hz, 3H, OCH_2CH_3). ^{13}C-NMR (100 MHz, DMSO-d_6, δ ppm): 165.80, 165.53, 155.17, 153.16, 152.88, 142.02, 140.95, 128.91, 127.22, 126.13, 124.54, 120.25, 108.67, 105.73, 61.95 (OCH_2CH_3), 61.25, 60.91, 60.56, 56.53, 56.44, 14.64 (OCH_2CH_3). Anal. calcd for $C_{24}H_{29}NO_9$ (475.49): C, 60.62; H, 6.15; N, 2.95. Found: C, 60.53; H, 6.22; N, 3.03.

*4.1.2.7 (Z)-Propyl 2-(3,4,5-trimethoxybenzamido)-3-(2,3,4-trimethoxyphenyl)acrylate (**6g**).* White powder (0.46 g, 63%), mp 111–113 °C. ^{1}H-NMR (400 MHz, DMSO-d_6, δ ppm): 9.88 (s, 1H, NH), 7.53 (s, 1H, olefinic CH), 7.46 (d, J = 8.9 Hz, 1H, arom. CH), 7.31 (s, 2H, arom. CH), 6.88 (d, J = 9.0 Hz, 1H, arom. CH), 4.11 (t, J = 6.4 Hz, 2H, $OCH_2CH_2CH_3$), 3.86 (s, 3H, OCH_3), 3.85 (s, 6H, $2OCH_3$), 3.80 (s, 3H, OCH_3), 3.76 (s, 3H, OCH_3), 3.74 (s, 3H, OCH_3), 1.63 (h, J = 7.2 Hz, 2H, $OCH_2CH_2CH_3$), 0.91 (t, J = 7.4 Hz, 3H, $OCH_2CH_2CH_3$). ^{13}C-NMR (100 MHz, DMSO-d_6, δ ppm): 165.91, 165.58, 155.18, 153.14, 152.89, 142.03, 140.91, 128.95, 127.26, 126.09, 124.56, 120.23, 108.69, 105.71, 66.64 ($OCH_2CH_2CH_3$), 61.94, 60.94, 60.56, 56.52, 56.44, 22.08 ($OCH_2CH_2CH_3$), 10.75 ($OCH_2CH_2CH_3$). Anal. calcd for $C_{25}H_{31}NO_9$ (489.51): C, 61.34; H, 6.38; N, 2.86. Found: C, 61.42; H, 6.29; N, 3.02.

*4.1.2.8 (Z)-Isopropyl 2-(3,4,5-trimethoxybenzamido)-3-(2,3,4-trimethoxyphenyl)acrylate (**6h**).* Pale yellow powder (0.44 g,

60%), mp 105–107 °C. ^{1}H-NMR (400 MHz, DMSO-d_6, δ ppm): 9.84 (s, 1H, NH), 7.47 (s, 1H, olefinic CH), 7.44 (d, J = 8.9 Hz, 1H, arom. CH), 7.30 (s, 2H, arom. CH), 6.87 (d, J = 9.0 Hz, 1H, arom. CH), 4.99 (dt, J = 12.5, 6.2 Hz, 1H, $OCH(CH_3)_2$), 3.85 (s, 3H, OCH_3), 3.85 (s, 6H, $2OCH_3$), 3.80 (s, 3H, OCH_3), 3.76 (s, 3H, OCH_3), 3.74 (s, 3H, OCH_3), 1.24 (d, J = 6.2 Hz, 6H, $OCH(CH_3)_2$). ^{13}C-NMR (100 MHz, DMSO-d_6, δ ppm): 165.83, 165.05, 155.10, 153.15, 152.85, 142.02, 140.90, 129.04, 126.86, 126.48, 124.54, 120.31, 108.66, 105.69, 68.70 ($OCH(CH_3)_2$), 61.94, 60.91, 60.56, 56.53, 56.43, 22.11 ($OCH(CH_3)_2$). Anal. calcd for $C_{25}H_{31}NO_9$ (489.51): C, 61.34; H, 6.38; N, 2.86. Found: C, 61.39; H, 6.44; N, 2.77.

*4.1.2.9 Butyl 2-(3,4,5-trimethoxybenzamido)-3-(2,3,4-trimethoxyphenyl)acrylate (**6i**).* White powder (0.39 g, 52%), mp 118–120 °C. ^{1}H-NMR (400 MHz, DMSO-d_6, δ ppm): 9.90 (d, J = 11.2 Hz, 1H, NH), 7.53 (d, J = 4.4 Hz, 1H, arom. CH), 7.44 (d, J = 8.8 Hz, 1H, arom. CH), 7.32 (d, J = 6.7 Hz, 2H, arom. CH), 6.87 (dd, J = 9.0, 1.8 Hz, 1H, arom. CH), 4.22–3.96 (m, 2H, $OCH_2CH_2CH_2CH_3$), 3.86 (s, 3H, OCH_3), 3.85 (s, 6H, $2OCH_3$), 3.80 (s, 3H, OCH_3), 3.76 (s, 3H, OCH_3), 3.74 (s, 3H, OCH_3), 3.74 (s, 2H, $OCH_2CH_2CH_2CH_3$), 1.64 (dt, J = 13.9, 7.0 Hz, 2H, $OCH_2CH_2CH_2CH_3$), 0.91 (t, J = 7.4 Hz, 3H, $OCH_2CH_2CH_2CH_3$). ^{13}C-NMR (100 MHz, DMSO-d_6, δ ppm): 166.10, 165.77, 155.23, 153.15, 152.91, 142.04, 141.00, 128.75, 127.48, 125.83, 124.55, 120.18, 108.68, 105.77, 66.65 ($OCH_2CH_2CH_2CH_3$), 61.96, 60.91, 60.57, 56.53, 56.45, 52.69 ($OCH_2CH_2CH_2CH_3$), 22.09 ($OCH_2CH_2CH_2CH_3$), 10.75 ($OCH_2CH_2CH_2CH_3$). Anal. calcd for $C_{26}H_{33}NO_9$ (503.54): C, 62.02; H, 6.61; N, 2.78. Found: C, 61.89; H, 6.67; N, 2.91.

4.2. Biological study

4.2.1. Antiproliferative activity on MCF-7 cells. Antiproliferative activity of the constructed acrylate molecules **5a–6i** was determined on MCF-7 cell line as reported previously.[38] See ESI Appendix A.†

4.2.2. Tubulin polymerization assay. The tubulin polymerization assay kit was used to measure the effect of the acrylate compounds **6e** and CA-4 on tubulin polymerization. See ESI Appendix A.†

4.2.3. Cell cycle analysis. The MCF-7 cell line was used for cell cycle analysis. Assay was carried out as reported previously.[39] See ESI Appendix A.†

4.2.4. Apoptosis assay. The MCF-7 cell line was used for Annexin V apoptosis assay. See ESI Appendix A.†

4.2.5. Impact on the expression levels of apoptosis related markers. The MCF-7 cell line was used for measurement of the expression levels of Apoptotic markers. See Section S4.2.5 in ESI.†

Conflicts of interest

The authors declare no conflict of interest.

References

1 P. Dhyani, C. Quispe, E. Sharma, A. Bahukhandi, P. Sati, D. C. Attri, A. Szopa, J. Sharifi-Rad, A. O. Docea, I. Mardare, D. Calina and W. C. Cho, Anticancer potential of alkaloids: a key emphasis to colchicine, vinblastine, vincristine, vindesine, vinorelbine and vincamine, *Cancer Cell Int.*, 2022, **22**, 206–213.
2 O. Ebenezer, M. Shapi and J. A. Tuszynski, A Review of the Recent Developments of Molecular Hybrids Targeting Tubulin Polymerization, *Int. J. Mol. Sci.*, 2022, **23**, 4001–4013.
3 L. Huang, Y. Peng, X. Tao, X. Ding, R. Li, Y. Jiang and W. Zuo, Microtubule Organization Is Essential for Maintaining Cellular Morphology and Function, *Oxid. Med. Cell. Longevity*, 2022, **2022**, 1623181–1623194.
4 A. K. E. Kiermaier, Dynamic Microtubule Arrays in Leukocytes and Their Role in Cell Migration and Immune Synapse Formation, *Front. Cell Dev. Biol.*, 2021, **9**, 1–18.
5 R. Vona, A. M. Mileo and P. Matarrese, Microtubule-Based Mitochondrial Dynamics as a Valuable Therapeutic Target in Cancer, *Cancers*, 2021, **13**, 5812.
6 H. A. J. Saunders, D. M. Johnson-Schlitz, B. V. Jenkins, P. J. Volkert, S. Z. Yang and J. Wildonger, Acetylated α-tubulin K394 regulates microtubule stability to shape the growth of axon terminals, *Curr. Biol.*, 2022, **32**, 614–630.e5.
7 B. Karahalil, S. Yardım-Akaydin and S. Nacak Baytas, An overview of microtubule targeting agents for cancer therapy, *Arh. Hig. Rada Toksikol.*, 2019, **70**, 160–172.
8 W. Liu, M. He, Y. Li, Z. Peng and G. Wang, A review on synthetic chalcone derivatives as tubulin polymerisation inhibitors, *J. Enzyme Inhib. Med. Chem.*, 2022, **37**, 9–38.
9 V. Čermák, V. Dostál, M. Jelínek, L. Libusová, J. Kovář, D. Rösel and J. Brábek, Microtubule-targeting agents and their impact on cancer treatment, *Eur. J. Cell Biol.*, 2020, **99**, 151075.
10 J. Yang, D. Song, B. Li, X. Gao, Y. Wang, X. Li, C. Bao, C. Wu, Y. Bao, S. Waxman, G. Chen and Y. Jing, Replacing the tropolonic methoxyl group of colchicine with methylamino increases tubulin binding affinity with improved therapeutic index and overcomes paclitaxel cross-resistance, *Drug Resistance Updates*, 2023, **68**, 100951–100962.
11 X.-L. Sun, Y.-R. Xie, N. Zhang, C.-T. Zi, X.-J. Wang and J. Sheng, Recent advances on small-molecule tubulin inhibitors, *Med. Res.*, 2021, **5**, 200024–200028.
12 T. Al-Warhi, L. S. Alqahtani, G. Alsharif, M. Abualnaja, O. A. Abu Ali, S. H. Qahl, H. A. E. Althagafi, F. Alharthi, I. Jafri, F. G. Elsaid, A. A. Shati, S. Aloufi, E. Fayad, I. Zaki and M. M. Morcoss, Design, Synthesis, and Investigation of Cytotoxic Activity of *cis*-Vinylamide-Linked Combretastatin Analogues as Potential Anticancer Agents, *Symmetry*, 2022, **14**, 2088.
13 Y. Lu, J. Chen, M. Xiao, W. Li and D. D. Miller, An Overview of Tubulin Inhibitors That Interact with the Colchicine Binding Site, *Pharm. Res.*, 2012, **29**, 2943–2971.
14 S. N. Baytas, Recent Advances in Combretastatin A-4 Inspired Inhibitors of Tubulin Polymerization: An Update, *Curr. Med. Chem.*, 2022, **29**, 3557–3585.
15 X. Yang, B. Cheng, Y. Xiao, M. Xue, T. Liu, H. Cao and J. Chen, Discovery of novel CA-4 analogs as dual inhibitors of tubulin polymerization and PD-1/PD-L1 interaction for

cancer treatment, *Eur. J. Med. Chem.*, 2021, **213**, 113058–113070.

16 X.-E. Jian, F. Yang, C.-S. Jiang, W.-W. You and P.-L. Zhao, Synthesis and biological evaluation of novel pyrazolo[3,4-*b*] pyridines as cis-restricted combretastatin A-4 analogues, *Bioorg. Med. Chem. Lett.*, 2020, **30**, 127025–127033.

17 M. A. Rahman, A. S. M. Saikat, M. S. Rahman, M. Islam, M. A. K. Parvez and B. Kim, Recent Update and Drug Target in Molecular and Pharmacological Insights into Autophagy Modulation in Cancer Treatment and Future Progress, *Cells*, 2023, **12**, 458–479.

18 R. G. D. Khodyuk, R. Bai, E. Hamel, E. M. G. Lourenço, E. G. Barbosa, A. Beatriz, E. D. A. dos Santos and D. P. de Lima, Diaryl disulfides and thiosulfonates as combretastatin A-4 analogues: Synthesis, cytotoxicity and antitubulin activity, *Bioorg. Chem.*, 2020, **101**, 104017–104024.

19 Z. Huo, K. Liu, X. Zhang, Y. Liang and X. Sun, Discovery of pyrimidine-bridged CA-4 CBSIs for the treatment of cervical cancer in combination with cisplatin with significantly reduced nephrotoxicity, *Eur. J. Med. Chem.*, 2022, **235**, 114271.

20 Z.-H. Chen, R.-M. Xu, G.-H. Zheng, Y.-Z. Jin, Y. Li, X.-Y. Chen and Y.-S. Tian, Development of Combretastatin A-4 Analogues as Potential Anticancer Agents with Improved Aqueous Solubility, *Molecules*, 2023, **28**, 1717.

21 E. Veignie, C. Ceballos, C. Len and C. Rafin, Design of New Antifungal Dithiocarbamic Esters Having Bio-Based Acrylate Moiety, *ACS Omega*, 2019, **4**, 4779–4784.

22 G. Verma, G. Chashoo, A. Ali, M. F. Khan, W. Akhtar, I. Ali, M. Akhtar, M. M. Alam and M. Shaquiquzzaman, Synthesis of pyrazole acrylic acid based oxadiazole and amide derivatives as antimalarial and anticancer agents, *Bioorg. Chem.*, 2018, **77**, 106–124.

23 I. Zaki, S. A. Eid, M. S. Elghareb, A.-S. M. Abas, G. Mersal and F. Z. Mohammed, In Vitro Antitumor Evaluation of Acrylic Acid Derivatives Bearing Quinolinone Moiety as Novel Anticancer Agents, *Anti-Cancer Agents Med. Chem.*, 2022, **22**, 1634–1642.

24 K. O. Mohamed, I. Zaki, I. M. El-Deen and M. K. Abdelhameid, A new class of diamide scaffold: Design, synthesis and biological evaluation as potent antimitotic agents, tubulin polymerization inhibition and apoptosis inducing activity studies, *Bioorg. Chem.*, 2019, **84**, 399–409.

25 N. E. A. A. El-Sattar, S. E. S. A. El-Hddad, M. M. Ghobashy, A. A. Zaher and K. El-Adl, Nanogel-mediated drug delivery system for anticancer agent: pH stimuli responsive poly(ethylene glycol/acrylic acid) nanogel prepared by gamma irradiation, *Bioorg. Chem.*, 2022, **127**, 105972–105981.

26 M. Hao, Y. Guo, Z. Zhang, H. Zhou, Q. Gu and J. Xu, 6-acrylic phenethyl ester-2-pyranone derivative induces apoptosis and G2/M arrest by targeting GRP94 in colorectal cancer, *Bioorg. Chem.*, 2022, **123**, 105802–105809.

27 F. A. R. Barbosa, M. P. Rode, R. F. Santos Canto, A. H. Silva, T. B. Creczynski-Pasa and A. L. Braga, Antiproliferative Effect and Autophagy Inhibition of Dihydropyrimidinone-Cinnamic Acid Hybrids, *ChemistrySelect*, 2022, **7**, e202200274.

28 B. Jayashree, P. S. Nikhil and S. Paul, Bioisosterism in Drug Discovery and Development-An Overview, *Med. Chem.*, 2022, **18**, 915–925.

29 I. Zaki, A. M. Y. Moustafa, B. Y. Beshay, R. E. Masoud, M. A. I. Elbastawesy, M. A. S. Abourehab and M. Y. Zakaria, Design and synthesis of new trimethoxylphenyl-linked combretastatin analogues loaded on diamond nanoparticles as a panel for ameliorated solubility and antiproliferative activity, *J. Enzyme Inhib. Med. Chem.*, 2022, **37**, 2679–2701.

30 O. W. V. Pongrakhananon, Post-translational modifications of tubulin: their role in cancers and the regulation of signaling molecules, *Cancer Gene Ther.*, 2023, **30**, 521–528.

31 T. Solomon, M. Rajendran, T. Rostovtseva and L. Hool, How cytoskeletal proteins regulate mitochondrial energetics in cell physiology and diseases, *Philos. Trans. R. Soc., B*, 2022, **377**, 20210324–20210332.

32 M. Hawash, Recent Advances of Tubulin Inhibitors Targeting the Colchicine Binding Site for Cancer Therapy, *Biomolecules*, 2022, **12**, 1843.

33 M. Mustafa, Y. A Mostafa, A. E. Abd Elbaky, M. Mohamed, D. Abdelhamid, E. MN Abdelhafez and O. M. Aly, Combretastatin A-4 analogs: Past, present, and future directions, *Octahedron Drug Res*, 2022, **1**, 55–64.

34 Q. Zhu, Y. A. An and P. E. Scherer, Mitochondrial regulation and white adipose tissue homeostasis, *Trends Cell Biol.*, 2022, **32**, 351–364.

35 H.-M. Zhou, J.-G. Zhang, X. Zhang and Q. Li, Targeting cancer stem cells for reversing therapy resistance: mechanism, signaling, and prospective agents, *Signal Transduction Targeted Ther.*, 2021, **6**, 62–74.

36 F. J. Bock and S. W. G. Tait, Mitochondria as multifaceted regulators of cell death, *Nat. Rev. Mol. Cell Biol.*, 2020, **21**, 85–100.

37 K. Cosentino, V. Hertlein, A. Jenner, T. Dellmann, M. Gojkovic, A. Peña-Blanco, S. Dadsena, N. Wajngarten, J. S. H. Danial, J. V. Thevathasan, M. Mund, J. Ries and A. J. Garcia-Saez, The interplay between BAX and BAK tunes apoptotic pore growth to control mitochondrial-DNA-mediated inflammation, *Mol. Cell*, 2022, **82**, 933–949.e9.

38 I. Zaki, M. K. Abdelhameid, I. M. El-Deen, A. H. A. Abdel Wahab, A. M. Ashmawy and K. O. Mohamed, Design, synthesis and screening of 1,2,4-triazinone derivatives as potential antitumor agents with apoptosis inducing activity on MCF-7 breast cancer cell line, *Eur. J. Med. Chem.*, 2018, **156**, 563–579.

39 M. K. Abdelhameid, I. Zaki, M. R. Mohammed and K. O. Mohamed, Design, synthesis, and cytotoxic screening of novel azole derivatives on hepatocellular carcinoma (HepG2 Cells), *Bioorg. Chem.*, 2020, **101**, 103995.